International Journal of GEOMATE, Oct., 2024 Vol.27, Issue 122, pp.54-62
ISSN: 2186-2982 (P), 2186-2990 (O), Japan, DOI: https://doi.org/10.21660/2024.122.4577
Geotechnique, Construction Materials and Environment

THERMAL CONDUCTIVITY AND VOLUMETRIC HEAT CAPACITY OF AIR-DRIED GRANULATED BENTONITE MIXTURES (GBMS) UNDER DIFFERENT PACKING CONDITIONS

Mazhar Nazir[1], Kengo Nakamura[2], Akihiro Matsuno[2], Toshihiro Sakaki[3] and *Ken Kawamoto[2]

[1]National Engineering Services Pakistan (Pvt.) Limited, Pakistan;
[2]Graduate School of Science and Engineering, Saitama University, Japan;
[3]ESE Consulting LLC, Japan

*Corresponding Author, Received: 07 May 2024, Revised: 13 Aug. 2024, Accepted: 29 Aug. 2024

ABSTRACT: Granulated bentonite mixtures (GBMs), crushed pellets mixed with powder to have a specific particle size distribution, have been validated as effective buffer materials for the geological disposal of radioactive waste due to their ease of transportation, in-situ placement and backfilling. The evaluation of heat transport parameters such as thermal conductivity (λ) and volumetric heat capacity (C) of GBMs is essential to assess the temperature distribution and its evolution with time and subsequent heat generated by the waste. Despite a large volume of studies on compacted bentonite including blocks, limited studies have been done for measuring λ and C of GBMs as well as examining the predictive models that are applicable to characterize those parameters under different packed conditions. In this study, therefore, the λ and C values of two GBM samples, FE-GBM used in the full-scale in-situ experiments in Switzerland and OK-GBM in Japan, packed with loose to dense conditions by controlling dry bulk density (DD), were measured at air-dried condition in the laboratory and the applicability of predictive existing models for λ and C has been tested. The results showed that the measured λ of FE-GBM gave slightly smaller values than those of OK-GBM at the same DD while there was no significant difference in the measured C values between two GBMs. The measured λ and C values for both GBMs increased linearly with increasing of DD, indicating simple linear regressions were applicable to represent the DD-dependence λ and C of GBMs in this study. These findings could be supported by the application of linear correlation models for both λ and C as a function of DD.

Keywords: Granulated Bentonite Mixtures (GBMs), Radioactive waste disposal, Thermal Conductivity, Heat Capacity, Dry bulk density

1. INTRODUCTION

Engineered barrier system (EBS) is one of the key elements in the widely-accepted concept of geological disposal of radioactive waste in deep geological formations. In most of the repository concepts, the waste would be contained in metal canisters surrounded by the buffer which is typically a layer of compacted clay (i.e., bentonite). To guarantee the long-term safety of a repository, all mechanisms that could affect the radionuclide migration rate must be well-defined and quantified [1]. Thermophysical properties of the buffer materials are the key parameters that control the rate of heat transfer from the waste dissipating into the surrounding rock mass. The heat released by the waste induces a thermal gradient through the bentonite buffer. Consequently, the coupled phenomena of thermal, hydraulic, mechanical, and geochemical processes occur during the transient period of the repository [2].

The bentonite buffer can take various forms. Highly compacted bentonite blocks were used to build the buffer in the full-scale engineered barriers experiment (FEBEX) at the Grimsel Test Site in Switzerland [3] and in the EBS experiment at the Horonobe Underground Research Center in Japan [4]. Both tests were full-scale in-situ demonstration experiments. There are other experiments for testing a different buffer concept based on granulated bentonite mixtures (GBMs). The GBMs refer particularly to crushed pellets mixed with powder to have a pre-specified particle size distribution. In this concept, canisters are placed on pedestals of highly compacted bentonite blocks, and the remaining space between the canisters and the tunnel wall is backfilled with the GBMs. This concept was realized in the Engineered Barrier (EB) experiment [5] and the Full-scale Emplacement (FE) experiment at the Mont Terri rock laboratory in Switzerland [6].

These full-scale in-situ experiments demonstrated that GBMs can be an effective buffer material for the geological disposal of radioactive waste due to easier transportation and in-situ emplacement than bentonite blocks. It is also known that GBMs yield a sufficient dry bulk density (DD) when properly manufactured and is superior in filling the spaces between the canister and irregular rock walls when emplaced properly [7]. Therefore, GBMs are highly adaptable for construction considering its practical

applications as well as economic perspectives.

There are a large number of studies for characterizing thermo-hydro-mechanical (THM) parameters of bentonite materials in the form of blocks, pellets, and power in the literature [8,9]. However, those focusing specifically on GBMs are limited, leading to a lack of knowledge. For properly interpreting and/or predicting the THM behavior in the GBMs, characterizing the material properties of GBMs (and possibly differentiating from those of blocks, pellets, and powders) is essential. The THM characteristics of bentonite are also known to be strongly associated with the microstructure [5,10]. As water inflow to the disposal tunnel causes the bentonite buffer to swell resulting in changes in the micropore structure, it is crucial to understand the process of *DD* change due to the expansion of GBMs [11]. Nazir et al. [12] evaluated the gas transport characteristics of two types of air-dried GBMs under different *DD* conditions (equivalently different microstructures). Gas transport processes through the GBMs were found to be highly controlled by pore structural parameters such as pore diameter, tortuosity, and pore connectivity.

As mentioned above, several studies have been done to characterize the thermal properties and to measure heat transport parameters for compacted bentonite (block-like). Limited studies, however, are to investigate the heat transport parameters for GBMs (granular-like) under different packed conditions. In this study, therefore, we aimed to measure the heat transport parameters such as thermal conductivity and volumetric heat capacity of air-dried GBMs under different packed conditions from loose to dense, and to examine the applicability of existing predictive models for the heat transport parameters.

2. MATERIALS AND METHODS

Granulated Bentonite Mixtures (GBMs) are mixtures of highly compressed pelletized/granulated material with various particle sizes, and often mixed with fines/powder. GBMs are manufactured to have relatively low initial water content of approximately 6% [13]. For typical bentonite blocks, on the other hand, DD = 1.65–1.80 g/cm^3 [14]. Pellets of bentonite processed at high pressure are compacted and milled typically to DD of 2.0 g/cm^3 or higher, 2.12 g/cm^3, and 2.18 g/cm^3 [13-16]. Unlike these forms of bentonite for which typical DD range is relatively narrow, the DD of GBMs vary over quite a wide range depending largely on the degree of compaction.

2.1 Material Preparation

Two types of GBMs, FE-GBM [13] and OK-GBM (trade name OK bentonite, Kunimine Industries, Japan) [17], were used to measure the heat transport parameters such as thermal conductivity (λ) and volumetric heat capacity (C) under differently packed conditions from loose to dense. The former GBM was used to fill the tunnel in the above-mentioned FE experiment whereas the latter is a commercial product.

Figure 1 shows photos of the two materials (FE-GBM and OK-GBM). The apparent color of the FE-GBM is grey, while that of the OK-GBM is whitish-grey. Both samples contain coarse and fine particles. The measured grain size distribution of the tested GBMs is shown in Fig. 2. The grain size distribution was prepared by sieving and mixing raw GBMs to follow so-called Fuller curve (with a maximum particle size of 6 mm and a shape factor of 0.4 to minimize inter-pellet porosity) and fall between pre-defined upper and lower boundaries [13].

Both materials (FE-GBM and OK-GBM) were stored in climate-controlled room under air-dried conditions (20℃ of temperature and 60% of relative humidity) to avoid any adverse influences from changes in the ambient relative humidity and/or temperature. Measurements of λ and C were conducted on these materials in the same air-dried conditions.

The basic physical and chemical properties of the two materials tests in this study, along with the values reported in the literature, are given in Table1 [12]. The average water content, as delivered, was 5.8 and 7.5 wt% for the FE-GBM and OK-GBM, respectively.

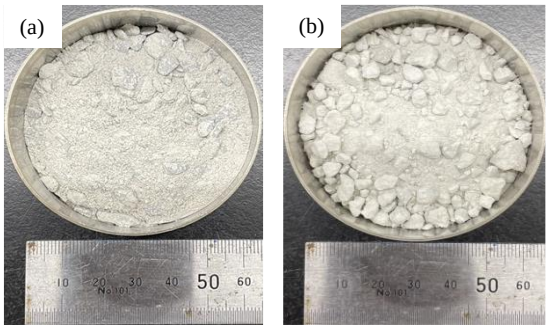

Fig.1 Photographs of the test materials. (a) FE-GBM and (b) OK-GBM

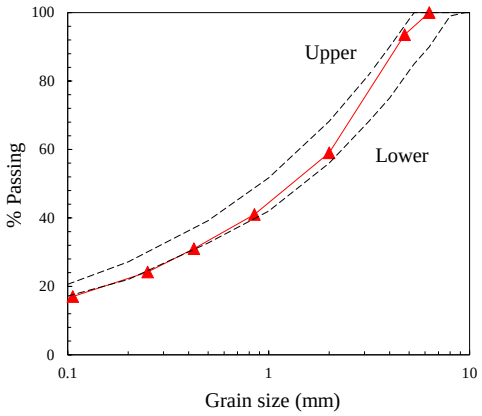

Fig.2 Grain size distribution of the tested materials, as well as upper and lower Fuller limit curves

Table 1. Basic physical and chemical properties of tested materials (after Nazir et al. [12])

Parameters	Unit	FE-GBM	OK-GBM
Specific gravity	-	2.72	2.62
Moisture content (Air-dry)	%	5.8	7.5
Specific surface area			
<0.106 mm	m^2/g	27.6	14.6
0.106-2 mm	m^2/g	26.8	152.1
Loss on Ignition	%	5.9	4.4
pH (1:10)	-	10.2	10.1
EC (1:10)	mS/cm	0.90	0.90
Mineralogy			
Montmorillonite	%	88-90	46-49
Quartz	%	7*	33*

**Typical values*

2.2 Packing of Materials

For the measurement of thermal conductivity and heat capacity, air-dried GBMs were hand-packed with different *DD*, ranging from loose to dense, into the acrylic core of 100 cm^3 (diameter of 5.61 cm and height of 4.06 cm). The FE-GBM were prepared at *DD* ranging from 1.25 to 1.75 g/cm^3, while the OK-GBM ranged from 1.09 to 1.75 g/cm^3. The samples were packed into the acrylic core without force at loose to medium *DD* conditions. The dense packed samples were prepared by tapping the samples with a small wooden rod.

2.3 Measurements of Thermal Conductivity and Heat Capacity

The heat transport parameters λ and C were measured by a portable thermal analyzer (KD2-Pro, Decagon Devices Inc, Pullman, WA, USA). The SH-1 sensor used in this study has two needles that are 30 mm in length, 1.3 mm in diameter, and 6 mm apart. With the needles inserted in the GBM samples, the applied heat at the heating needle transfers through the GBM sample and is monitored by the other needle during the heating period followed by a cooling period. From the recorded data of the heat dissipation in the sample, the values of λ and C were determined. For each *DD* condition, triplicate measurements were taken, and the average λ and C values were analyzed.

3. PREDICTIVE MODELS FOR THERMAL CONDUCTIVITY AND HEAT CAPACITY

There are a number of models for predicting heat transport parameters of soils and rocks from various viewpoints such as porosity, moisture content, and constituents [18,19]. Among those predictive models, four models for λ, and two for C, described below were selected due to their easy and simple applicability was evaluated statistically. Additionally, simple linear regressions obtained from measured data in this study were also used (see Fig. 3 & 5).

3.1 Thermal conductivity

3.1.1 Woodside and Messmer model

Woodside and Messmer model [20] was proposed based on the geometric mean of the three components (solid, water, and air) and was originally developed for determining electrical conductivity. The model assumes three parallel heat flow paths in an idealized unit cube of soil. It consists of a path of width through fluid and solid in parallel, a path of width through continuous solid material, and a path of width through continuous pore fluid. Given the thermal conductivity and volume fractions of each component, the bulk or apparent thermal conductivity can be determined as:

$$\lambda = \lambda_s^{(1-\Phi)} \lambda_w^{\Phi Sr} \lambda_a^{\Phi(1-Sr)} \quad (1)$$

where λ_x is the thermal conductivity of each phase [x: solid (s), water (w), and air (a)] (W m^{-1} K^{-1}), Φ is the total porosity (cm^3 cm^{-3}), S_r is the degree of saturation in soil (-).

For water and air, typical values at room temperature λ_w = 0.57 W m^{-1} K^{-1} and λ_a = 0.025 W m^{-1} K^{-1} were used. The values of λ_s for FE-GBM and OK-GBM were calculated from the geometric mean of minerals composition reported by [12]. For FE-GBM, quartz = 7% and other minerals = 93%, thus λ_s = $7.7^{0.07} \times 2^{0.93}$ = 2.2 W m^{-1} K^{-1}. For OK-GBM, quartz = 33 % and other minerals = 67%, thus λ_s = $7.7^{0.33} \times 2^{0.67}$ = 3.12 W m^{-1} K^{-1}.

3.1.2 de Vries model

de Vries model [21] used the volumetric fractions and λ of each soil constituent (solids, water, and air), and the weighting factors describing the shape and orientation of soil particles and air pores:

$$\lambda = \frac{\theta\lambda_w + F_a\varepsilon\lambda_a + F_s\sigma\lambda_s}{\theta + F_a\varepsilon + F_s\sigma} \quad (2)$$

where θ is the volumetric water contents (cm^3 cm^{-3}) and ε is the air-filed porosity (= 1-θ; cm^3 cm^{-3}). The parameters F_s and F_a are the weighing factors for the shape and orientation of soil particles and pores, respectively. F_s and F_a are given as:

$$F_a = \frac{1}{3}\left[\frac{2}{1+\left(\frac{\lambda_s}{\lambda_w}-1\right)\times g_a} + \frac{1}{1+\left(\frac{\lambda_s}{\lambda_w}-1\right)\times g_c}\right] \quad (3)$$

$$F_S = \frac{1}{3}\left[\frac{2}{1+\left(\frac{\lambda_s}{\lambda_w}-1\right)\times 0.125} + \frac{1}{1+\left(\frac{\lambda_s}{\lambda_w}-1\right)\times 0.75}\right] \quad (4)$$

$$g_a = 0.333 - \frac{\varepsilon}{\Phi}(0.333 - 0.035);\ for\ 0.09 \le \theta \le \Phi \quad (5)$$

$$g_a = 0.013 + 0.944\theta; for\ 0 \le \theta \le 0.09 \quad (6)$$

$$g_c = 1 - 2g_a \quad (7)$$

3.1.3 Campbell model for thermal conductivity

Campbell [22] suggested the λ estimation model of soils based on the following empirical equation derived by McInnes [23]:

$$\lambda = A + B\theta - (A - D)\exp\left[-(C\theta)^E\right] \quad (8)$$

where *A*, *B*, *C*, *D*, and *E* are the coefficients obtained by curve fitting. The Campbell model related these coefficients to soil properties as described below:

$$A = 0.65 - 0.78DD + 0.60DD^2 \quad (9)$$

$$B = 1.06DD \quad (10)$$

$$C = 1 + \frac{2.6}{{m_c}^{0.5}} \quad (11)$$

$$D = 0.03 + 0.1DD^2 \quad (12)$$

$$E = 4 \quad (13)$$

where m_c is the clay mass fraction of the soil (=1 g/g for GBMs in this study).

3.1.4 Tang model

Tang et al. [24] proposed a linear correlation model to estimate λ of compacted MX80 bentonite as a function of air-filled porosity (ε) based on their experimental data. They found that this linear relationship also predicted λ of other compacted bentonites (e.g., FEBEX and Kunigel) with a reasonable accuracy:

$$\lambda = \alpha\varepsilon + \lambda_0 \quad (14)$$

where α is the fitted slope of λ vs. ε, λ_0 is the λ at ε = 0.

3.2 Heat Capacity

3.2.1 Farouki model

Farouki [25] examined different methods based on their experimental results to calculate the volumetric heat capacity (*C*) and suggested the predictive equation:

$$C = \frac{DD}{W_D}\left(0.18 + 1.0 \times \frac{w}{100}\right)C_w \quad (15)$$

where W_D is the wet density of soil (g/cm^3), *w* is the water content of soil (%), and C_w is the specific heat of the water (= 4.18 J g^{-1} K^{-1}).

3.2.2 Campbell model for heat capacity

Campbell [26] suggested an estimation model based on the volumetric heat capacity of each soil constituent:

$$C = C_w\rho_w\theta + C_sDD \quad (16)$$

where C_s is the specific heat capacity of solid (J g^{-1} K^{-1}) (FE-GBM: 0.865 J g^{-1} K^{-1}, OK-GBM: 0.846 J g^{-1} K^{-1} [12]). C_w is the specific heat of water (= 4.18 J g^{-1} K^{-1}).

3.3 Statistical Analysis

The performance of above-mentioned predictive models was evaluated by two statistical parameters such as root mean square error (RMSE) and bias. The RMSE describes the over mode fitted to the measured data. The bias indicates the model's overestimation or underestimation as compared to the measured data:

$$\text{RMSE} = \sqrt{\frac{1}{n}\sum_{i=1}^{n} d_i^2} \quad (17)$$

$$\text{bias} = \frac{1}{n}\sum_{i=1}^{n} d_i \quad (18)$$

where d_i is the difference between the measured and predicted i^{th} values. *n* is the number of measurements in the data set.

4. RESULTS AND DISCUSSION

4.1 Measurement of Thermal Conductivity

The measured values of thermal conductivity (λ) of GBMs as a function of dry bulk density (*DD*) and air-filled porosity (ε) are shown in Fig. 3. For both FE-GBM and OK-GBM, in general, the λ values increased quasi-linearly with increasing *DD* and decreased quasi-linearly with increasing ε. At *DD* = 1.75 g cm^{-3} of OK-GBM, the measured λ turned out significantly high (the value circled in a broken line in Fig. 3). Based on the visual observation, it was presumed that the high λ value resulted likely from the breakage of the granules as quite high compaction energy was required to achieve this *DD* (i.e., the GBM property became close to bentonite block (see Fig. 4). This data point was excluded from the fitting of a linear relationship.

Even though the measured λ values of OK-GBM were higher than those of FE-GBM at the same *DD* and ε, there was no significant difference between the slopes in λ (*DD* or ε) for both air-dried samples in this study. This is likely because OK-GBM had a higher fraction of quartz (with high λ_s) of 33% and water content of 7.52% than those for FE-GBM (7% quartz, 5.84% water content). The *DD* (solid phase ratio) dependence on λ for air-dried GBM samples was similar to each other.

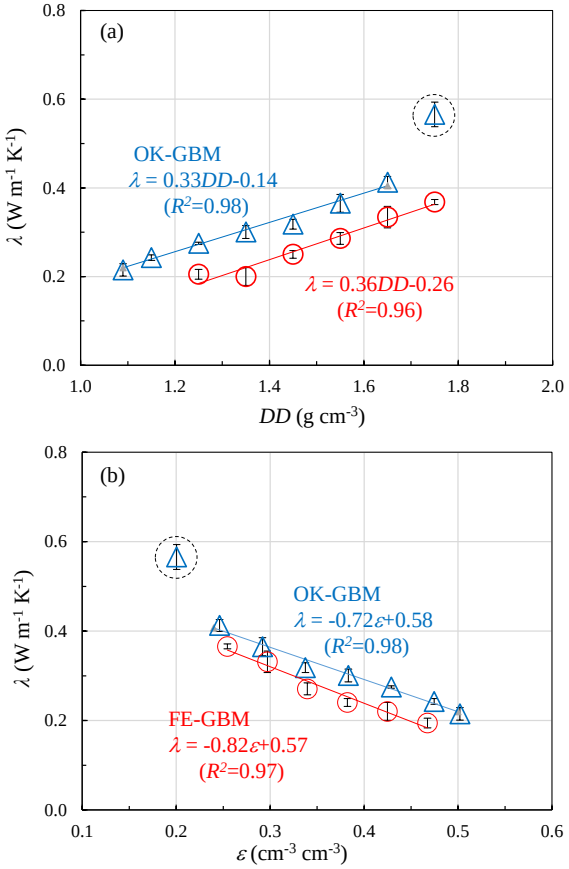

Fig.3 Measured thermal conductivity (λ) as a function of (a) dry bulk density (DD) and (b) air-filled porosity (ε)

The measured λ values as a function of DD in this study were compared to those of previously reported bentonite materials as shown in Fig. 4. In the figure, the bentonite materials were categorized into i) GBMs and powders and ii) compacted bentonite and blocks. The measured λ of FE-GBM and OK-GBM in this study were consistent with the results for similar Wyoming GBM [27]. As the compaction of FE-GBM and OK-GBM proceeded, the λ values approached those of the highly compacted samples reported by Tang and Cui [28]. In general, GBMs are to be produced with relatively low water content. Consequently, the measured thermal conductivity of GBMs covered the corresponding range of lower DD with lower water content than those of highly compacted blocks. In this range, the thermal conductivity was somewhat less dependent to the DD. However, it is noteworthy that, as it was compressed to a higher degree, the thermal conductivity well blended/merged to that of the blocks.

As described in Section 2, GBMs can take a wide range of DD compared to bentonite in other forms. The measured DD of FE-GBM used in this study ranged from 1.25 to 1.75 g/cm^3. This was consistent with the DD range of GBMs measured at the tunnel wall (1.3-1.8 g/cm^3) in the full-scale demonstration test using GBM, as reported by Sakaki et al. [6,27]. The measured DD of OK-GBM was from 1.1 to 1.75 g/cm^3. Therefore, GBMs exhibited a wide range of DD including that below 1.5 g/cm^3 that have not been considered for blocks or pellets, and down to that of powder. The λ values of GBMs showed a low sensitivity to DD under approximately 1.5 g/cm^3, but for DD > 1.5 g/cm^3, the λ values increased significantly with DD. It is implied that as the DD of GBMs increases, the fines get compressed/densified and the gas phase decreases, which enhances the bridging effects by the fine grains between the large pellets so that more heat can flow.

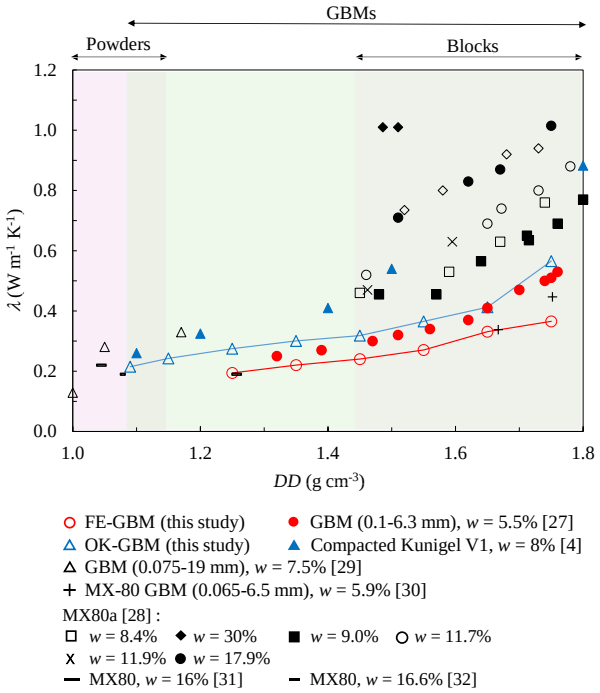

Fig.4 Comparison of measured thermal conductivity (λ) with the literature values

4.2 Measurement of Heat Capacity

The measured volumetric heat capacity (C) of the GBMs presented as a function of DD and ε in Fig. 5, increased linearly with increasing DD and decreased linearly with increasing of ε. There was no significant difference between the linear regressions in $C(DD)$ and $C(\varepsilon)$ for both GBMs in this study, indicating that the differences in the mineral composition and initial water content between the two air-dried GBMs did not affect bulk C of the tested samples. It was confirmed that DD mainly controlled the measured bulk C for the range of DD considered in this study.

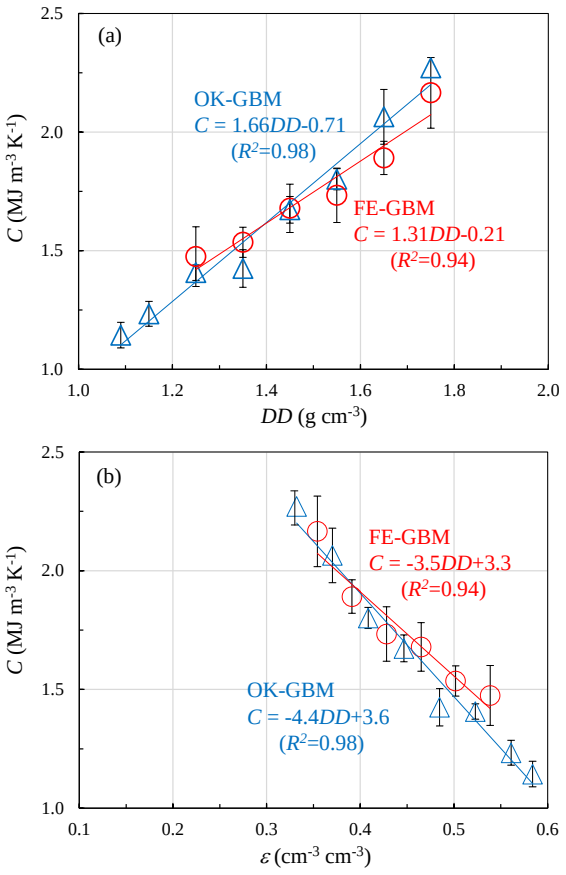

Fig.5 Measured heat capacity (C) as a function of (a) dry bulk density (DD) and (b) air-filled porosity (ε)

4.3 Characteristics of Thermal Conductivity and Heat Capacity with Change of Dry Bulk Density

As noted above, GBMs take a wide range of DD. Therefore, it exhibits different thermal conductivity (λ) and heat capacity (C) depending on the forms of bentonite materials. The strong dependency of the measured λ and C on DD is often explained by the distribution of liquid and solid phases. In the case of low DD of GBMs, the fine grains and pellets are mixed with each other (Fig. 1) with different thermophysical properties. In the case of higher DD in the GBMs, the fine grains will eventually have the same density of the pellets, and the contact between them will also be denser (i.e. enhanced bridging effect), resulting in uniform thermophysical properties in the GBMs.

From the change in DD of GBMs, FE-GBM has a higher DD from the beginning compared to OK-GBM and is less likely to compress more. OK-GBM is in contact with fine grains and liquid and solid phases as it is compacted with increasing DD. For GBMs with DD < 1.5 g/cm^3, the thermal conductivities do not differ significantly. It is thought that this is because the fine grains of GBMs are not sufficiently compacted, and thus have their own thermal conductivity and characteristics with a gas phase.

At DD comparable to compacted bentonite blocks (> 1.5 g/cm^3), the thermal conductivity of GBMs had a slope similar to that of bentonite blocks. This may be correlated with the homogenization within the GBM and fine grains (granules) induced by the compaction at high DD facilitated the increase of bulk λ of air-dried GBMs in this study. The measured C, on the other hand, was not significantly different between the FE-GBM and OK-GBM used in this study (Fig. 5) and the measured C of both samples increased solely with increasing DD and decreased with increasing air-filled porosity. Again, this indicated that the differences in the mineral composition and initial water content of GBMs did not affect the bulk C and the DD simply controlled the bulk C of air-dried GBMs.

4.4 Performance of Predictive Models

The scatterplot comparisons of the predicted and measured values of λ and C are shown in Figs. 6 and 7. The calculated values of RMSE and bias for the predictive λ and C models are summarized in Table 2. In the table, the RMSE and bias calculated for the linear relationships fitted in this study are also given for comparison. For λ in Fig. 6, the predicted values by different models ranged roughly between the 1:2.5 and 1.5:1 lines in the scatterplots for both FE-GBM and OK-GBM. The linear-type model [24] yielded the best performance in predicting the λ measured in this study. For C in Fig. 7, on the other hand, the Campbell model [26] predicted better than that of Farouki model [25] and the predicted values ranged mostly between 1:1.1 and 1.25:1 for FE-GBM and ranged between 1:1.25 to 1.25:1 for OK-GBM. In accordance with the scatterplot in Fig. 7, a linear-type model gave a better performance (smaller RMSE and bias) in estimating C than the other model as shown in Table 2.

These findings suggested that, for the GBMs compacted at air-dried conditions that have the same grain size distribution (Fig. 2), a simple linear-type predictive model would be applicable to predict both λ and C values, irrespective of the difference in the mineral composition. In the present study, only two GBMs have shown this DD-dependent thermal characteristics. Further studies are needed to validate the characteristics observed in this study by changing the grain size distribution and testing different type of bentonite grain materials.

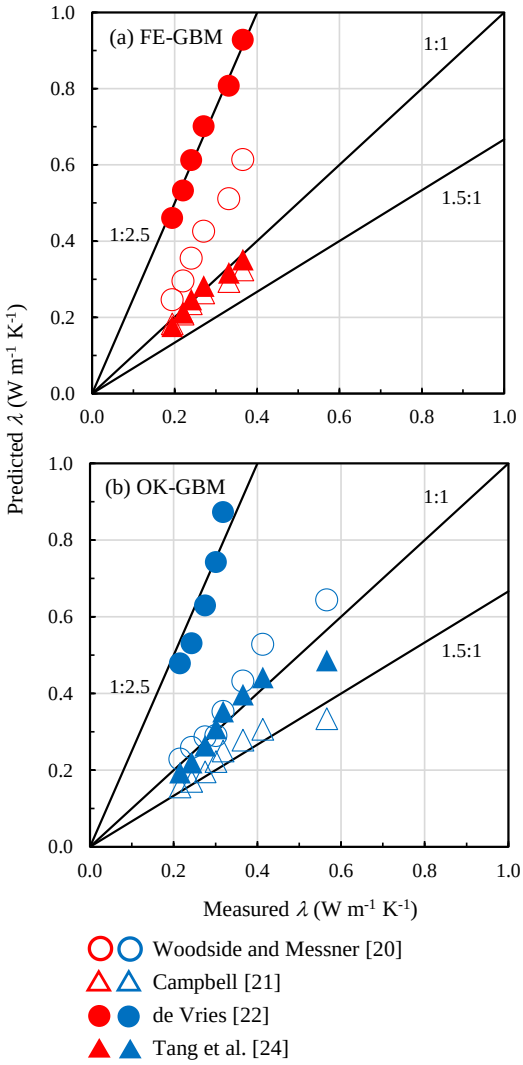

Fig.6 Scatterplot comparison of the predicted and measured thermal conductivity (λ)

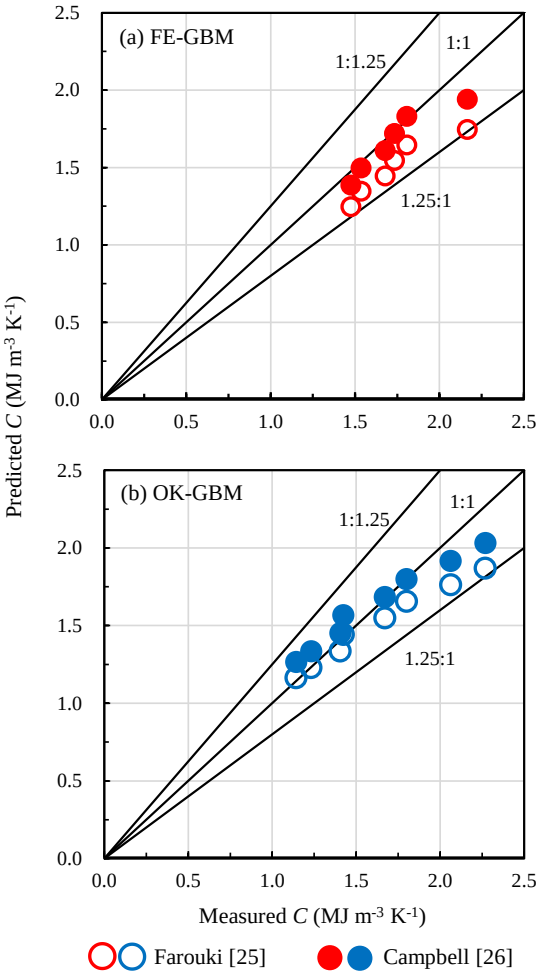

Fig.7 Scatterplot comparison of the predicted and measured heat capacity (C)

Table 2. RMSE and Bias for the predictive thermal conductivity (λ) and heat capacity (C) models

Model	FE-GBM		OK-GBM	
Thermal conductivity, λ	RMSE	bias	RMSE	bias
Woodside and Messmer [20]	0.23	0.18	0.15	0.14
de Vries [21]	0.42	0.40	0.56	0.52
Campbell [22]	0.024	-0.02	0.11	-0.10
Tang et al. [24]	0.019	0.01	0.036	0.014
Linear regression (This study)	0.015	-0.01	0.009	-0.003
Volumetric heat capacity, C	RMSE	bias	RMSE	bias
Farouki [25]	0.26	-0.25	0.19	-0.13
Campbell [26]	0.11	-0.08	0.13	0.003
Linear regression (This study)	0.06	0.008	0.06	-0.005

5. CONCLUSIONS

In this paper, thermal conductivity (λ) and volumetric heat capacity (C) of two GBMs, FE-GBM and OK-GBM, were measured under a wide range of dry bulk density (DD) conditions from loose to dense. Because of their relatively low water content, and DD range covering lower values than bentonite blocks, they showed different characteristics (i.e. less dependency to the DD) than those of typical highly compacted bentonite and blocks.

The measured λ of FE-GBM gave slightly smaller values than those of OK-GBM at the same DD, probably due to the difference of quartz content between two GBMs. The measured C values, on the other hand, there was no significant difference between two GBMs in the range of packed DD in this study. For both GBMs, the measured λ and C values increased with increasing of DD. The increment of measured λ values was smaller compared to those of bentonite blocks. This may be due to the three-phase

change, resulting from the change of internal granular forms (e.g. breakage of the pellets).

For both λ and C, the linear-type model predicted well the measured λ and C values of GBMs in this study. This suggests that a simple linear model would be applicable to estimate the λ and C for practical application when we predict the heat flow in GBMs under variably packed conditions. Because it can be understood that the change of *DD* due to the compaction of grains directly affects the λ and C, it is an important challenge to correlate the microstructural analysis (e.g. visualization of transitional change with increasing of *DD*) with measured heat transport parameters as well as the moisture-induced microstructural change of grains (e.g. swelling) for future studies.

6. ACKNOWLEDGMENTS

This work was made possible by the 'Providing New Insight into Interactions Between Soil Functions and Structure' (PROTINUS)-project in the framework of 2020. The authors are thankful to NAGRA, Switzerland for providing the FE-GBM to carry out this research work.

7. REFERENCES

[1] Villar, M. V., Carbonell B., Martín P, L. and Gutiérrez-Álvares C., The role of interfaces in the bentonite barrier of a nuclear waste repository on gas transport, Engineering Geology, Vol. 286, 2021, 106087.

[2] Gens, A., Garitte B., Olivella S. and Vaunat J., Applications of multiphysical geomechanics in underground nuclear waste storage, European Journal of Environmental and Civil Engineering, Vol. 13(7-8), 2011, pp. 937-962.

[3] Alberdi, J., Barcala J.M., Campos R., Cuevas A. M. and Fernandez E., FEBEX project: Full-scale engineered barriers experiment for a deep geological repository for high level radioactive waste in crystalline host rock, Report No.: ENRESA--1/2000, 2000, pp. 1-362.

[4] Suzuki, H. and Takayama Y., Impact assessment of density change on the buffer material on the coupled thermal-hydraulic and mechanical (THM) behavior in the near-field, JAEA-Research, 2020, pp. 1-52 (in Japanese).

[5] Alonso E.E., Romero E. and Hoffmann C., Hydromechanical behavior of compacted granular expansive mixtures: Experimental and constitutive study, Géotechnique, Vol. 61, Issue 4, 2011. pp. 329–344.

[6] Sakaki, T., Firat Lüthi B. and Vogt, T., Investigation of the emplacement dry density of granulated bentonite mixtures using dielectric, mass-balance and actively heated fiber-optic distributed temperature sensing methods, Geomechanics for Energy and the Environment, Vol. 32, 2022, 100329.

[7] Villar, M.V., Iglesias R.J., Gutiérrez-Álvarez C. and Carbonell B., Pellets/block bentonite barriers: Laboratory study of their evolution upon hydration, Engineering Geology, Vol. 292, Issue 2, 2021, 106272.

[8] Zhu, J., Su Z. and Zhang H, Soil-water characteristic curves and hydraulic conductivity of Gaomiaozi bentonite pellet-contained materials, Environmental Earth Sciences, Vol. 81, Issue 3, 2022, 92.

[9] Fattah, M.Y., Salim N.M. and Irshayyid E.J., Determination of the soil-water characteristic curve of unsaturated bentonite-sand mixtures, Environmental Earth Science, Vol. l76, 2017, 201.

[10] Romero, E. and Simms, P.H., Microstructure investigation in unsaturated Soils: A review with special attention to contribution of mercury intrusion porosimetry and environmental scanning electron microscopy, Geotechnical and Geological Engineering, Vol. 26, Issue 6, 2008, pp. 705-727.

[11] Gens, A. and Sánchez M., Long-term Performance of Engineered Barrier Systems PEBS, DELIVEERABLE (D-N°:D3.5-2), Formulation of a model suitable for long term predictions, European Commission, 2010, pp. 1-24.

[12] Nazir, M., Kawamoto K., Sakaki T., Komatsu T. and Moldrup P., Gas transport parameters of differently compacted granulated Bentonite mixtures (GBMs) under air-dried conditions, Soil and Foundations, Vol. 62, Issue 6, 2022, 101223.

[13] Garitte, B., Weber H. and Müller H.R., Requirements, Manufacturing and QC of the Buffer Components Report, LUCOEX-WP2, Deliverable (D-N°:D2.3), 2015.

[14] Mokni, N., Cabrera J. and Deleruyelle F., On the installation of an in situ large-scale vertical SEALing (VSEAL) experiment on bentonite pellet-powder mixture, Journal of Rock Mechanics and Geotechnical engineering, Vol. 15, Issue 7, 2023, pp. 2388-2401.

[15] Villar, V.M., Iglesias, J.R., Gutiénrrez-Álvarez C. and Carbonell B., Pellets/block bentonite barriers: Laboratory study of their evolution upon hydration, Engineering Geology, Vol. 292, Issue 2, 2021, 106272.

[16] Hoffmann, C., Alonso E.E. and Romero E., Hydro-mechanical behavior of bentonite pellet mixtures, Physics and Chemistry of the Earth, Vol. 32, Issues 8-14, 2007, pp. 832-849.

[17] Nakashima, H., Saito A. and Ishii T., Method for producing high-density bentonite pellets using

dry shrinkage, Journal of Nuclear Fuel Cycle and Environment, Vol. 21, Issue 2, 2014, pp. 83-94 (in Japanese).
[18] He, H., He D., Jin J., Smits K.M., Dyck M., Wu Q., Si B. and Lv J., Room for improvement: A review and evaluation of 24 soil thermal conductivity parameterization schemes commonly used in land-surface, hydrological, and soil-vegetation-atmosphere transfer models, Earth-Science Reviews, Vol. 211, 2020, 103419.
[19] Kodešová, R., Vlasáková M., Fér M., Teplá D., Jakšík O., Neuberger P. and Adamovsky R., Thermal properties of representative soils of the Czech Republic, Soil & Water Research, Vol. 8, Issue 4, 2013, pp. 141-150.
[20] Woodside, W. and Messmer, J.H., 1961, Thermal conductivity of porous media. II Consolidated Rocks, Journal of Applied Physics, Vol. 32, Issue 9, 1961, pp. 1699–1706.
[21] de Vries. D.A., Thermal properties of soil, Physics of Plant Environment, W. R. van Wijk (Ed), North-Holland Publishing Company, 1963, pp. 210-235.
[22] Campbell, G.S., Soil Physics with BASIC: Transport Models for Soil-Plant Systems, Developments in Soil Science, Elsevier Science Ltd., Vol. 14, 1985, pp. 1-149.
[23] McInnes, K.J., Thermal conductivities of soils from dryland wheat regions of Eastern Washington. M.Sc. Washington State University, 1981, pp. 1-102.
[24] Tang, A., Cui, Y. J. and Le, T.T., A study on the thermal conductivity of compacted bentonites, Applied Clay Science, Vol. 41, 2008, pp. 181-189.
[25] Farouki, O.T., Thermal Properties of Soil, Defense technical report, 1981, pp. 1-136
[26] Campbell, G.S., Calissendorff C. and Williams J.H., Probe for measuring soil specific heat using a heat pulse method, Soil Science Society of America Journal, Vol. 55, Issue 1, 1991, pp. 291-293.
[27] Sakaki, T., Firat Lüthi B., Vogt T., Uyama M. and Niunoya S., Heated fiber-optic cables for distributed dry density measurements of granulated bentonite mixtures: Feasibility experiments, Geomechanics for Energy and the Environment, Vol. 17, 2019, pp. 57-65.
[28] Tang, A. and Cui Y.J., Determining the thermal conductivity of MX-80 clay, Fourth International Conference on Unsaturated Soils, 2006, pp. 1695-1706.
[29] Masuda, R., Asano H., Toguri S., Mori T., Shimura T., Matsuda T., Uyama M. and Noda M., Buffer construction technique using granular bentonite, Journal of Nuclear Science and Technology, Vol. 44, Issue 3, 2007, pp. 448-455.
[30] Wieczorek K., Czaikowski O. and Miehe R., PEBS - Long-term performance of engineered barrier system, GRS 353, Gesellschaft für Anlagenund Reaktorsicherheit (GRS) gGmbH, 2014, pp. 1-127.
[31] Marjavaara, P., Holt R. and Sjönlom V., Customized bentonite pellets: Manufacturing, performance and gap filling properties, Working report 2012-62, 2013, pp. 1-70.
[32] Kivikoski, H., Heimonen I. and Hyttinen H., Bentonite pellet thermal conductivity techniques and measurements, Posiva Working Report, Vol. 9, 2015, pp. 1-50.